# Illuminating structural transformation of Ir(110): A high-temperature scanning tunneling microscopy study

J. J. Schulz,[1,2] M. Sturmat,[2] and R. Koch[1]

[1]*Paul-Drude-Institut für Festkörperelektronik, Hausvogteiplatz 5-7, D-10117 Berlin*
[2]*Institut für Experimentalphysik, Freie Universität Berlin, Arnimallee 14, D-14195 Berlin*

High-temperature scanning tunneling microscope investigation of Ir(110) reveals that the originally {331} faceted room-temperature surface flattens upon heating to form $(1\times3)+(1\times1)$ and eventually $(1\times2)$ missing row reconstructed terraces at about 800 K, thus finally resolving a long-standing controversy on its equilibrium configuration. The surprising structural transformations can be explained by a surface stress related mechanism that is consistent also with the reconstruction behavior of the other low index planes of the noble metals.

The equilibrium arrangement of surface atoms is one of the intriguing issues of scientific branches as different as catalysis, thin-film epitaxy, surface science and, in particular, surface dynamics, crystallography, and others. Due to the reduced number of chemical bonds both the interatomic equilibrium distances and the equilibrium geometry at the surface may differ from the bulk. The charge redistribution in metallic surface layers normally favors shorter bond lengths, thus generating tensile stress, when the surface atoms remain in registry with the bulk.[1,2]

The low index planes of the noble metals Au, Pt, and Ir constitute an extraordinary group of surfaces. Here the tendency to contract is so strong that even the close-packed (111) planes reconstruct to obtain a denser surface mesh.[3,4] For instance, in the well-known herringbone superstructure of Au(111) an extra row of atoms is inserted every 23 rows.[5,6] On Pt(111) an analogous reconstruction has been observed at temperatures above 1330 K,[7] or as low as 400 K when the chemical potential of Pt was raised.[8] Ir(111) seems to be stable in the bulk truncated geometry.[9] Interestingly also the square (001) surfaces of Au, Pt, and Ir reconstruct to form buckled quasihexagonal, i.e., (111)-like overlayers. The simplest geometry is found on Ir(001), which exhibits a $(1\times5)$ superstructure with an additional atom row inserted every five lattice distances.[10]

The obvious trend towards surface densification seems to be counteracted at the more open (110) surfaces [Fig. 1(a)]. Both Au(110) and Pt(110) exhibit the well known $(1\times2)$ missing row (MR) structure at room temperature, where every second close-packed row of the topmost layer is missing [Fig. 1(b)];[11] compared with bulk the atomic density therefore is not increased but halved. In the case of Ir(110) the situation is even more complex: Earlier studies favored also a $(1\times2)$ MR reconstruction as for Au and Pt,[12–14] or a $(1\times3)$ MR structure [Fig. 1(c)] mixed with $(1\times1)$ patches [Fig. 1(a)].[15–18] More recent investigations, however, are in support of a faceted equilibrium configuration characterized by mesoscopic ridges with {331} facets as side planes (Fig. 2).[19–21]

Here we report on a high-temperature STM (scanning tunneling microscope) study of Ir(110), which finally solves this intricate puzzle. We will show that the originally {331} faceted surface flattens upon heating to form $(1\times3)+(1\times1)$ and eventually $(1\times2)$ MR reconstructed terraces at about 800 K, thus demonstrating that quenched states have been investigated in the previous room-temperature studies. On basis of these interesting experimental results a surface stress related mechanism is proposed which explains the surprising temperature dependent structural transformation of Ir(110). The mechanism is in accordance with present theory and moreover consistent with the reconstruction behavior of the low index planes of Au, Pt, and Ir, in general.

The experiments were performed in a UHV chamber with a base pressure of $5\times10^{-11}$ h Pa, equipped with a home-built variable temperature UHV-STM, a four-grid retarding field analyzer for LEED (low-energy electron diffraction) and AES (Auger electron spectroscopy) as well as the usual facilities for sample preparation (for details see Ref. 22). The Ir(110) sample—exhibiting a miscut of less than 0.3°—was prepared by repeated cycles of Ne sputtering at 830 K and
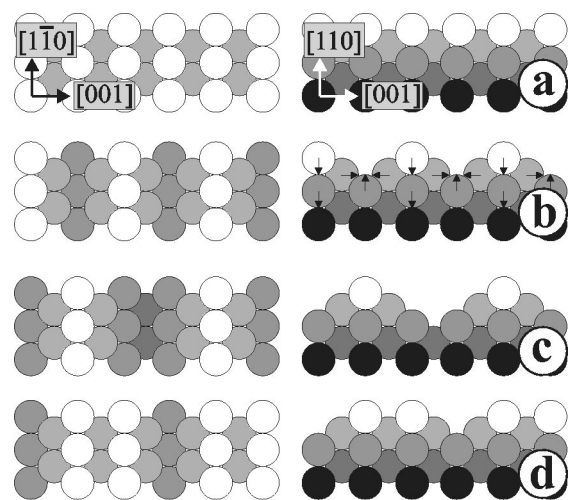


FIG. 1. Hard-sphere models in top (left) and side view representation (right) of (a) fcc(110), (b) the fcc(110)$(1\times2)$ MR reconstruction, (c) and (d) two possible of fcc(110)$(1\times3)$ MR configurations; in (b) the directions of the experimentally determined atom shifts are indicated (see text).
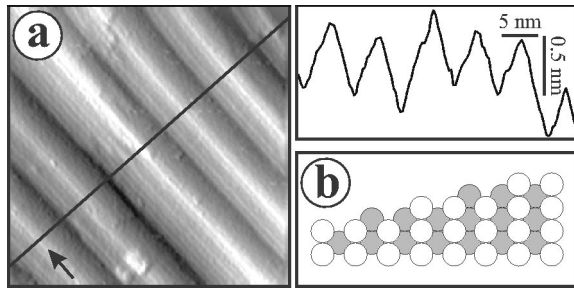
FIG. 2. (a) $28\times28$-nm$^2$ STM image of Ir(110) at $300\pm5$ K showing a faceted morphology with ridges parallel to the $[1\bar{1}0]$ direction (marked by arrow) and {331} facets as side planes; single scan is along the solid line in the top view; $U_T=526$ mV, $I_T=5$ nA. (b) Hard-sphere model of {331} facets in side view representation.

flashing to 1250 K. Our results are not influenced by the oxygen pretreatment of the sample during preparation. The same results are obtained irrespective whether small amounts of oxygen were dosed after sputtering or not. The STM images were taken in the constant current mode with chemically etched tungsten tips. To enhance contrast the experimental height values are superposed by the partial derivation along the fast scanning direction (corresponding to an artificial illumination effect).

In accordance with previous studies[19–21] the Ir(110) surface exhibits a faceted morphology at room temperature; it is characterized by 0.5–1.5-nm high ridges that extend several 100 nm in the $[1\bar{1}0]$ direction. The STM image of Fig. 2(a) shows single ridges, where the close-packed rows of the {331} facets [compare sphere model of Fig. 2(b)] as well as occasionally even monosteps on the facets are clearly resolved.

When the temperature is increased, the surface flattens. At 520 K it consists of small (110) terraces which predominantly are $(1\times3)$ reconstructed [Fig. 3(a)]; in addition, though to a lesser amount, also small unreconstructed, i.e., $(1\times1)$ patches are observed [Fig. 3(b)]. The $(1\times3)$ MR structure which is usually referred to in the literature exhibits fully developed {111} nanofacets as illustrated in Fig. 1(c). However, the corrugation of the $(1\times3)$ periodicity determined experimentally is only $\approx0.04$ nm (compare single scan of Fig. 3). Since this value is considerably lower than the $\approx0.14$ nm expected for the $(1\times3)$ MR structure of
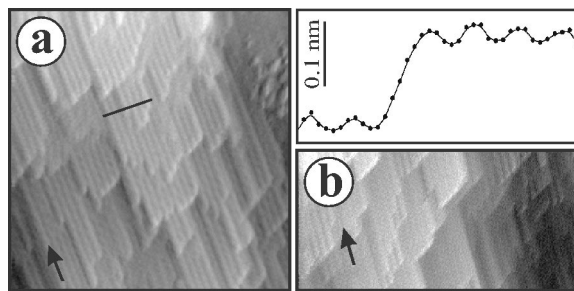


FIG. 3. STM image of Ir(110), taken at $520\pm20$ K: (a) $44\times44$ nm$^2$, showing small (110) terraces which predominantly are $(1\times3)$ MR reconstructed; single scan is along the solid line in the top view; (b) $44\times22$ nm$^2$, showing additionally also small unreconstructed patches; $U_T=526$ mV, $I_T=2$ nA.
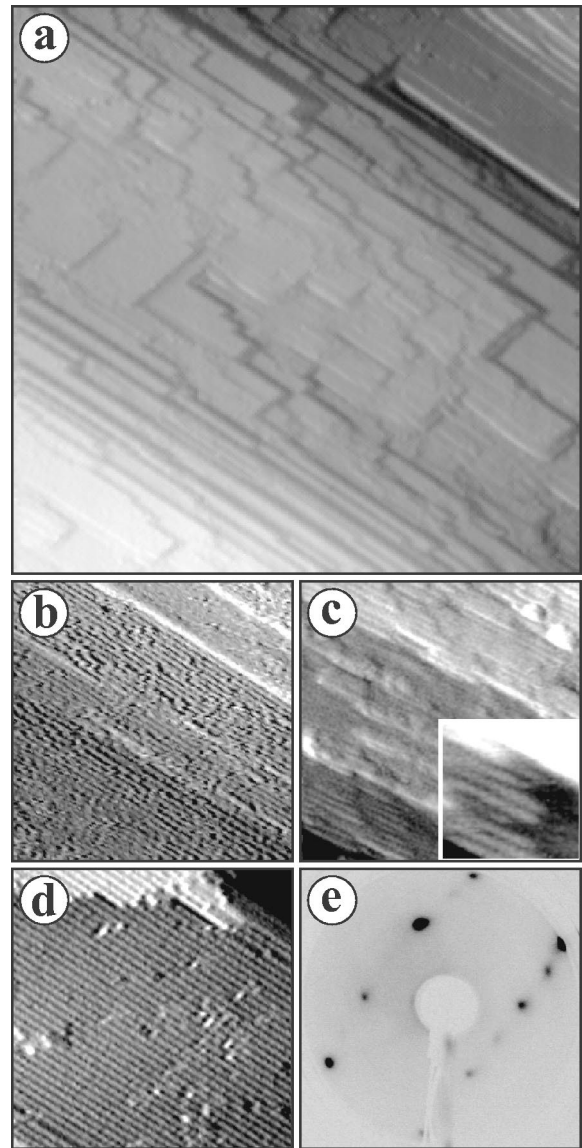


FIG. 4. (a) $90\times90$-nm$^2$ STM image of Ir(110) taken at $890\pm50$ K revealing extended (110) terraces; $U_T=-499$ mV, $I_T=4$ nA. (b) High magnification STM image, also taken at 890 K, where the $(1\times2)$ MR reconstruction of the terraces is resolved; $U_T=-526$ mV, $I_T=3$ nA. (c) $40\times40$-nm$^2$ STM image taken at $790\pm40$ K, $U_T=526$ mV, $I_T=5$ nA. (d) $28\times28$-nm$^2$ STM image ($U_T=-68$ mV, $I_T=3.2$ nA), and (e) LEED image of the quenched $(1\times2)$ MR structure of Ir(110), both taken below 400 K.

Fig. 1(c),[23] our STM results (see also below) seem to be in favor of a more shallow MR configuration. The MR model of Fig. 1(d) with two close packed rows separated by only one row missing represents a possible atomic arrangement which is intermediate between the {331} facetted ridges observed at room temperature and the $(1\times2)$ MR reconstruction developed upon further heating (see below); on the one hand it can be regarded as the smallest possible {331} facet structure or, on the other hand, as a succession of $(1\times2)$ MR and $(1\times1)$ units.

When the temperature is raised to 890 K, extended (110) terraces are observed [Fig. 4(a)]. As revealed by high mag-

nification STM images, taken at the same temperature [e.g., Fig. 4(b)], the reconstruction of the terraces has changed to a $(1 \times 2)$ MR structure compared with 520 K. These surprising findings are corroborated by in situ LEED investigation at 890 K. Instead of the streaky LEED patterns usually obtained at room temperature (see Ref. 19) distinct $(1 \times 2)$ spots are detected.[24] By rapidly cooling the sample below 400 K the $(1 \times 2)$ MR configuration can be quenched with high quality. STM image and LEED pattern of the quenched sample [Fig. 4(d) and (e)] still exhibit sharp half order diffraction spots as well as the 0.8 nm periodicity, respectively, thus confirming the occurrence of a $(1 \times 2)$ MR reconstruction at 890 K. Figure 4(c) shows the sample after extended thermalization at 790 K. At this lower temperature only small $(1 \times 2)$ MR domains have developed (see inset).

The structural transformation performed by Ir(110), when the temperature is raised, indeed is surprising. Whereas Au(110) and Pt(110) undergo roughening transitions in the same temperature range,[25] the morphology of Ir(110) transforms from a faceted, i.e., rough, to a reconstructed flat state. The reconstructed phases occurring at elevated temperatures, i.e., $(1 \times 3) + (1 \times 1)$ and $(1 \times 2)$ MR, were observed already at room temperature in previous studies[12–18] and considered as the respective equilibrium configurations. However, our results reveal that obviously frozen-in surface configurations have been investigated in these studies, which is further corroborated by the quenching experiment of Fig. 4. On the other hand, when the cooling of the sample proceeds slowly within a time period of about one hour, the structural transformation is reversible recovering again the facetted morphology at room temperature. We remark that the appearance of a $(1 \times 3)$ MR phase at elevated temperatures was observed also in the ion scattering study by Heiland's group;[26] the reported temperature range of 540–800 K is in excellent agreement with our findings. In order to exclude impurities as origin of the restructuring, which may affect the surface charge density, we checked the contamination level of our sample. In accordance with previous studies[19–21] the contamination at room temperature was beyond the detection limit of our analyzer and did not change upon heating.

How can we understand the strange behavior of Ir(110) compared with the other two noble metals? As discussed above the low index planes of the noble metals, in particular the (111) and (001) surfaces exhibit a strong tendency to form hexagonal, i.e., (111)-like atom configurations. Atoms of the (111) surface are already arranged hexagonally and moreover occupy energetically favorable fcc sites. Therefore the driving force for the formation of a denser surface mesh, partially with energetically unfavorable hcp stacking, certainly is the reduction of tensile surface stress as confirmed theoretically.[3,4] The atomic density of Au(111) herringbone superstructure is increased by 4.3% compared with the bulk (111) plane. In the case of the (001) surfaces the situation is more complicated. Because the geometry changes from square to hexagonal upon reconstruction, relief of surface stress is not the only relevant parameter.[27] It is interesting, however, that the atomic density of the hexagonal $(1 \times 5)$ overlayer [e.g., of Ir(001)] again is increased by approximately 4% compared to bulk (111). The neighboring $(1 \times 4)$ and $(1 \times 6)$ reconstructions with five and seven

atomic rows at distances of four and six (001) lattice units, respectively, are not observed experimentally; the atomic density in these reconstructions is increased by 8 and 1%, respectively. On the more open (110) surfaces insertion of an additional atom row between the close-packed rows requires a densification of about 20% compared to bulk (111). Here the strain obviously is too high to establish a continuous buckled (111)-like layer on the (110) surfaces. Therefore the surface realizes densification and hexagonal configuration locally via formation of {111} nanofacets of the $(1 \times 2)$ MR structure. The vertical distance of the topmost layer is reduced by about 20% in the case of Au(110) and Pt(110), the atom rows of the second layer are shifted laterally as sketched in Fig. 1(b).[30] Relief of tensile surface stress indeed has been identified as driving force by first-principle calculations in the case of Pt(110)$(1 \times 2)$,[28] but not for Ir(110). According to Filippetti and Fiorentini[29] the tensile stress is even higher in the $(1 \times 2)$ MR reconstructed than in the unreconstructed surface.

In order to explain the restructuring of Ir(110) we make the plausible assumption that—analogous to Pt(110)—the $(1 \times 2)$ MR reconstruction of Ir(110) observed above 800 K is stabilized by the reduction of tensile surface stress. It is well known that the equilibrium atomic distances shrink, when the temperature decreases. Since the thermal vibrational amplitudes of the surface atoms usually are larger, the thermal expansion of the surface is enhanced compared with bulk.[31,32] Consequently, upon cooling, the surface shrinks faster than the bulk. The row pairing of the second layer [compare Fig. 1(b)] therefore is gradually reduced until there is eventually enough space to have the missing row inserted again and the surface deconstructs. Of course, the deconstructed surface is still under surface stress favoring the formation of a stepped configuration, where stress relief is facilitated. The preferred formation of intrinsically stepped {331} facets therefore is a natural compromise between deconstruction and stress relaxation. We note that our interpretation is confirmed by previous room temperature LEED intensity analysis[14] of presumably quenched (!) Ir(110) $\times(1 \times 2)$; according to this study the side shift of the second layer atoms is only half as large for Ir(110) than for Au(110) or Pt(110),[30] thus facilitating the refilling of the missing row. Higher-order $(1 \times n)$ MR structures as discussed in theoretical studies[33,29] seem to be energetically unfavorable, because stress relaxation is obstructed on larger {111} facets. A surface stress related mechanism explains also the different reconstruction behavior observed in field ion microscopy (FIM) studies compared to the single-crystal experiments on extended flat terraces. The FIM studies unanimously report the formation of $(1 \times 2)$ MR reconstruction at about 500 K on the (110) nanofacets of field emitter tips.[34–36] Since the contractive forces of the facets at the tip side slightly expand the lattice of the (110) facet, the $(1 \times 2)$ MR is stabilized already at lower temperatures by the mechanism discussed above.

In conclusion, with our high-temperature STM investigation of Ir(110) we discovered that the surface transforms from a {331} facetted morphology at room temperature to a flat $(1 \times 2)$ MR reconstructed configuration at about 800 K.

The structural transformation can be consistently explained-with a mechanism relying on temperature-dependent surface stress as driving force. Our study for the first time provides a unifying picture which reconciliates the many at first sight contradictory experiments on the equilibrium configuration of Ir(110) as well as the reconstruction behavior of the low index planes of the noble metals, in general.

[1] R.J. Needs, Phys. Rev. Lett. **58**, 53 (1987).

[2] H. Ibach, Surf. Sci. Rep. **29**, 193 (1997).

[3] S. Narasimhan and D. Vanderbilt, Phys. Rev. Lett. **69**, 1564 (1992).

[4] R.J. Needs, M.J. Godfrey, and M. Mansfield, Surf. Sci. **242**, 215 (1991).

[5] C. Wöll, S. Chiang, R.J. Wilson, and P.H. Lippel, Phys. Rev. B **39**, 7988 (1989).

[6] J.V. Barth, H. Brune, G. Ertl, and R.J. Behm, Phys. Rev. B **42**, 9307 (1990).

[7] A.R. Sandy, S.G.J. Mochrie, D.M. Zehner, G. Grübel, K.G. Huang, and D. Gibbs, Phys. Rev. Lett. **68**, 2192 (1992).

[8] M. Bott, M. Hohage, T. Michely, and G. Comsa, Phys. Rev. Lett. **70**, 1489 (1993).

[9] C.-M. Chan, S.L. Cunningham, M.A. van Hove, W.H. Weinberg, and S.P. Withrow, Surf. Sci. **66**, 394 (1977).

[10] N. Bickel and K. Heinz, Surf. Sci. **163**, 435 (1985).

[11] R. Koch, M. Borbonus, O. Haase, and K.H. Rieder, Appl. Phys. A: Solids Surf. **55**, 417 (1992), and references therein.

[12] K. Christmann and G. Ertl, Z. Naturforsch. **28A**, 1144 (1973).

[13] J.L. Taylor, D.E. Ibbotsen, and W.H. Weinberg, Surf. Sci. **79**, 349 (1979).

[14] M.A. van Hove, W.H. Weinberg, and C.-M. Chan, in *Low-Energy Electron Diffraction*, Springer Series in Surface Science Vol. 6 (Springer, Berlin, 1986).

[15] W. Hetterich and W. Heiland, Surf. Sci. **210**, 129 (1989).

[16] H. Bu, M. Shi, F. Masson, and J.W. Rabalais, Surf. Sci. **230**, L140 (1990).

[17] M. Shi, H. Bu, and J.W. Rabalais, Phys. Rev. B **42**, 2852 (1990).

[18] W. Hetterich, H. Niehus, and W. Heiland, Surf. Sci. **264**, L177 (1992).

[19] R. Koch, M. Borbonus, O. Haase, and K.H. Rieder, Phys. Rev. Lett. **67**, 3416 (1991).

[20] W.F. Avrin and R.P. Merrill, Surf. Sci. **274**, 231 (1992).

[21] J. Kuntze, S. Speller, and W. Heiland, Surf. Sci. **402**, 764 (1998).

[22] O. Haase, M. Borbonus, P. Muralt, R. Koch, and K.H. Rieder, Rev. Sci. Instrum. **61**, 1480 (1990).

[23] G. Binnig, H. Rohrer, Ch. Gerber, and E. Weibel, Surf. Sci. **131**, L379 (1983).

[24] Visual inspection of the *in situ* LEED patterns of the 890-K hot sample indeed reveals sharp $(1 \times 2)$ reflections irrespective of the beam energy. Because of the large background radiation of the glowing sample these images are not shown here.

[25] R. Koch, M. Sturmat, and J.J. Schulz, Surf. Sci. **454-456**, 543 (2000), and references therein.

[26] W. Hetterich, C. Höfner, and W. Heiland, Surf. Sci. **251/252**, 731 (1991).

[27] A. Filippetti and V. Fiorentini, Surf. Sci. **377-379**, 112 (1997).

[28] P.J. Feibelman, Phys. Rev. B **51**, 17 867 (1995).

[29] A. Filippetti and V. Fiorentini, Phys. Rev. B **60**, 14 366 (1999).

[30] E. Vlieg, I.K. Robinson, and K. Kern, Surf. Sci. **233**, 248 (1990), and references therein.

[31] K. Pohl, J.-H. Cho, K. Terakura, M. Scheffler, and E.W. Plummer, Phys. Rev. Lett. **80**, 2853 (1998).

[32] T. Miyake, I. Oodake, and H. Petek, Surf. Sci. **427-428**, 39 (1999).

[33] K. W. Jacobsen and J. K. Nørskov, in *The Structure of Surfaces II*, Springer Series of Surface Science Vol. 11, edited by J. van der Veen and M. A. van Hove (Springer, Berlin, 1988), p. 118.

[34] J.D. Wrigley and G. Ehrlich, Phys. Rev. Lett. **44**, 661 (1980).

[35] G.L. Kellogg, J. Vac. Sci. Technol. A **5**, 747 (1987).

[36] Q. Gao and T.T. Tsong, Phys. Rev. B **36**, 2547 (1987).